2013 IEEE 10th International Symposium on Biomedical Imaging:
From Nano to Macro
San Francisco, CA, USA, April 7-11, 2013

VESSEL WALKER : CORONARY ARTERIES SEGMENTATION USING RANDOM WALKS AND HESSIAN-BASED VESSELNESS FILTER

Faten M'hiri(1), *Luc Duong*(1), *Christian Desrosiers*(1), *Mohamed Cheriet*(2)

École de technologie supérieure
Departement of Software and IT Engineering(1)
Department of Automated Manufacturing Engineering(2)
1100 Notre-Dame St. W., Montreal, Canada

ABSTRACT

The segmentation of vascular structures from 2D X-ray angiographies is an important step for vessel measurement, diagnosis and treatment planning. Segmentation of such structures can be challenging due to the vessel appearance and topology. In this paper, we propose a novel interactive method to segment vascular structures by combining Hessian-based vesselness information and the random walk formulation, in which manually selected seed points can be used to refine the segmentation result. The proposed method was tested on coronary arteries angiograms and has shown to be more accurate than an active contour-based method or the Random Walker algorithm, with a mean AUC of 97.2%.

***Index Terms*—** Vessel segmentation, angiographies, random walks, graph cuts, coronary arteries

1. INTRODUCTION

According to the World Health Organization, cardiovascular diseases such as coronary heart disease are the first worldwide cause of death [1]. To diagnose and treat these diseases, minimally invasive percutaneous interventions like balloon angioplasty are often preferred over open-heart surgery, due to their shorter operation and recovery times, and their reduced risk of postoperative complications. In balloon angioplasty, coronary vessels are revascularized by inserting a catheter in the affected coronary and inflating a balloon to put a stent in place. This intervention is routinely conducted under biplane or monoplane fluoroscopic guidance, where a contrast agent such as iodine is injected at key moments to enhance the coronary vessel lumen diameter. The images produced by this process are known as X-ray angiographies.

One of the major challenges during navigation in the coronary arteries is that the contrast agent cannot be continuously injected in the targeted vessel because of its toxicity. To provide guidance under low contrast, coronary vessels can be outlined using segmentation. The segmentation of vascular structures, which can also be used for vessel measurement, diagnosis and treatment planning, is a highly challenging task due to the wide range of vessel sizes, shapes and intensities, to the complex topology including vessel bifurcations and overlap, and to local deformations such as aneurysms or stenoses.

The problem of segmenting vessel-like structures is well documented in the literature (e.g., see [2] for a comprehensive survey). Among the solutions proposed for this problem are vesselness filters [3, 4], which estimate the vessel centerness probability of pixels using the spectral properties of the Hessian matrix, at various scales. Because such filters do not consider connectivity information, the segmentation obtained by thresholding their output is often composed of many disconnected regions. Also, these filters may have difficulty detecting smaller vessels or local deformations to the vessel, for instance, caused by aneurysms. More complex approaches have been developed to overcome the limitations of vesselness filters, including methods based on region growing [5] and active contours [6]. Although such methods have the ability to obtain well-connected regions, they are often sensitive to the placement of initial seeds and the complex topology of the coronary arteries (e.g., bifurcations and small vessels). Graph-based methods, using minimal paths [7], random walks [8] and graph cuts [9, 10, 11], have also been proposed. In many of these approaches, like [9] and [10], intensity values are used as class priors of pixels or voxels. In angiograms, however, this information is unreliable since smaller vessels can have the same intensities as the background.

In this paper, we present a new vessel segmentation approach that extends the random walks formulation of [8] by integrating vesselness information. While recent works have also proposed to combine vesselness with graph cuts [10, 11], our approach offers several advantages. Thus, unlike [11] where vesselness values are thresholded to generate seeds, our method uses these values directly in the energy function, which makes it more robust to the tubular structures in the background (false positives). Moreover, our method may also use manually entered seeds to refine the segmentation

This research was funded by a grant from *Fonds de recherche du Quebec Nature et technologies* FQRNT (http://www.fqrnt.gouv.qc.ca/).

of smaller vessels or noisy regions. In [10], seeds are only considered in a post-processing step and can not be used to remove background noise. Finally, as mentioned in [8], methods based on random walks may be preferable in some cases, since they are less sensitive to the shrinking bias problem.

2. PROPOSED METHOD

As in other graph-based approaches, our method considers the input image $\mathcal{I}$ as a graph where nodes are pixels, and a pixel i is connected to the pixels in its neighborhood $\mathcal{N}_i$. For instance, $\mathcal{N}_i$ can be defined as the pixels within a certain distance of i. Each edge (i, j) has a weight w_{ij} expressing the similarity of intensity between pixels i and j, computed as

$$w_{ij} \;=\; \begin{cases} \exp\big(-\gamma\,(\mathcal{I}_i - \mathcal{I}_j)^2\big), & \text{if } j \in \mathcal{N}_i \\ 0, & \text{otherwise,} \end{cases} \tag{1}$$

where $\mathcal{I}_i$ represents the intensity level of pixel i, and parameter γ controls how intensity differences affect the weights.

For each pixel i, we also have a class prior $b_i \in [0, 1]$ representing the vesselness of i as defined in Frangi's filter [3]. Vesselness values are obtained by comparing the minimum and maximum curvatures around i, given by the first and second eigenvalues of the Hessian matrix at i, λ_{i1} and λ_{i2}. Pixels within vessel-like structures will have a low curvature along the vessel and a high curvature across it. Following Frangi's formulation, we compute these values as

$$b_i \;=\; \begin{cases} 0, & \text{if } \lambda_{i2} > 0 \\ \exp\Big(-\frac{R^2}{2\mu_R^2}\Big)\Big(1 - \exp\big(\frac{S^2}{2\mu_S^2}\big)\Big) & \text{otherwise,} \end{cases}, \tag{2}$$

where $R = \lambda_{i1}/\lambda_{i2}$, $S = \sqrt{\lambda_{i1}^2 + \lambda_{i2}^2}$, and μ_R, μ_S are parameters controlling the filter's response. To take into account the different vessel sizes, the filter is applied at different scales and the highest obtained response is kept for each pixel.

Given a set of seeds $\mathcal{S}$, we search for a mapping $\boldsymbol{f} : \mathcal{I} \to \{0, 1\}$ such that $f_i = 1$ if pixel i is in a vessel, and $f_i = 0$ if i is a background pixel. This mapping should satisfy the seed labels, i.e. $f_i = s_i, \forall s_i \in \mathcal{S}$, and should minimize the following energy function:

$$\begin{aligned} E(\boldsymbol{f}) \;=& \frac{1}{2}\sum_{i=1}^{|\mathcal{I}|}\sum_{j=1}^{|\mathcal{I}|} w_{ij}(f_i - f_j)^2 \;+\; \alpha\sum_{i=1}^{|\mathcal{I}|}(1 - b_i)f_i^2 \\ &+\; \beta\sum_{i=1}^{|\mathcal{I}|} b_i(f_i - 1)^2. \end{aligned} \tag{3}$$

The first term of the function minimizes the total weight of cut edges (i.e., edges connecting a foreground pixel to a background one), while the second and third terms respectively minimize the vesselness of background pixels and maximize vesselness of foreground pixels. Parameters $\alpha, \beta \geq 0$ are used to control the trade-off between these three components.

Let W be the matrix of weights w_{ij} and D be the diagonal matrix such that $[D]_{ii} = \sum_j w_{ij}$. The Laplacian matrix of $\mathcal{I}$ can be defined as $L = D - W$. Moreover, denote by $\boldsymbol{b}$ the vector of vesselness values b_i, and let B be a diagonal matrix such that $[B]_{ii} = b_i$. The energy function can be expressed in matrix form as

$$E(\boldsymbol{f}) \;=\; \boldsymbol{f}^\top M \boldsymbol{f} \;-\; 2\beta\boldsymbol{b}^\top\boldsymbol{f} \;+\; \beta\boldsymbol{b}^\top\mathbf{1}, \tag{4}$$

where $M = L + \alpha I + (\beta - \alpha)B$.

To consider the seeds, we reorder the pixels of $\mathcal{I}$ in two groups containing labeled and unlabeled pixels. Denote by $\boldsymbol{f}_U$ the mapping of unlabeled pixels and by $\boldsymbol{f}_L$ the mapping of labeled ones. We can then rewrite Equation (4) as

$$\begin{aligned} E(\boldsymbol{f}) \;=& \left[\begin{array}{c|c} \boldsymbol{f}_U^\top & \boldsymbol{f}_L^\top \end{array}\right] \left[\begin{array}{c|c} M_{UU} & M_{UL} \\ \hline M_{UL}^\top & M_{LL} \end{array}\right] \left[\begin{array}{c} \boldsymbol{f}_U \\ \hline \boldsymbol{f}_L \end{array}\right] \\ &-\; 2\beta \left[\begin{array}{c|c} \boldsymbol{b}_U^\top & \boldsymbol{b}_L^\top \end{array}\right] \left[\begin{array}{c} \boldsymbol{f}_U \\ \hline \boldsymbol{f}_L \end{array}\right] \;+\; \beta\boldsymbol{b}^\top\mathbf{1}. \end{aligned} \tag{5}$$

The optimal segmentation can then be obtained by relaxing the integer constraints on $\boldsymbol{f}$, deriving this energy function with respect to variables $\boldsymbol{f}_U$ and setting the result to zero, yielding the following solution:

$$\boldsymbol{f}_U \;=\; M_{UU}^{-1}\Big(\beta\boldsymbol{b}_U - M_{UL}\boldsymbol{f}_L\Big). \tag{6}$$

While seeds can be used to refine the segmentation in regions where the vesselness response is unreliable, the proposed method can also be used without any seeds. In this fully automatic approach, the solution can be obtained as

$$\boldsymbol{f} \;=\; \beta\big(L + \alpha I + (\beta - \alpha)B\big)^{-1}\boldsymbol{b}. \tag{7}$$

Moreover, when the vesselness values of background and foreground pixel are equally important, i.e. if $\alpha = \beta$, the solution further simplifies to

$$\boldsymbol{f} \;=\; \alpha\big(L + \alpha I\big)^{-1}\boldsymbol{b}, \tag{8}$$

In this case, α can be seen as a regularization parameter which pulls the solution toward the values returned by the vesselness filter.

Once $\boldsymbol{f}$ has been computed, the pixels can be classified as background or foreground by thresholding the values of $\boldsymbol{f}$. A good threshold value can be found automatically using Otsu's algorithm [12], which looks for the threshold that minimizes the weighted within-class variance.

3. RESULTS AND DISCUSSION

Our proposed segmentation approach was evaluated on 9 different patient angiograms. Parameters were empirically selected on a separate validation dataset, and set to $\gamma = 850$ and

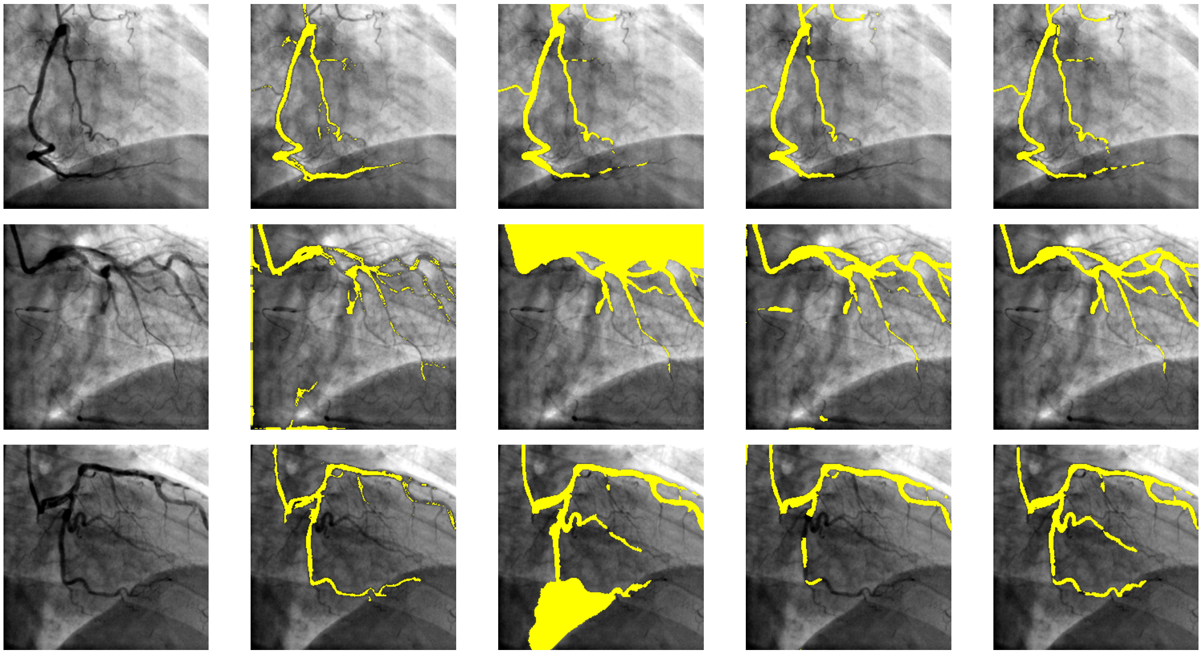

Fig. 1. Segmentation results obtained with automatic thresholding. From left to right: Original images, Active Contour results, Random Walker results and our proposed method using the fully automated and the semi-automatic formulations.

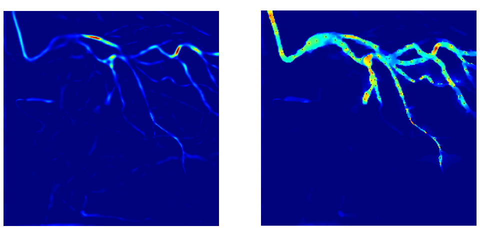

Fig. 2. Foreground class probabilities obtained by Frangi's filter (*left*) and our proposed method (*right*).

$\alpha = \beta = 0.2$ for the semi-automatic formulation (VW-SA) as presented in Equation (6) and $\alpha = 0.05$ and $\beta = 0.5$ for the automatic formulation (VW-A) of Equation (7). While the choice of these parameters may depend on the nature of the image and its contrast, we found our method to work well with a wide range of values. Furthermore, a 5×5 pixel neighborhood was used for our tests. Although larger neighborhoods may facilitate the diffusion of information across noisy regions, they also lead to denser Laplacian matrices, which increases the computation time and memory requirements. To detect both small and large vessels, Frangi's filter scales ranging from $\sigma_{min} = 1$ to $\sigma_{max} = 3$ where used. In the semi-automatic approach, about 100 pixels, on average, were manually labeled (as background or foreground seeds) per image (out of the 65536 pixels), representing $1-3$ minutes of work for an untrained user. These seeds were useful mostly for the segmentation of low contrast regions (e.g., small vessels) and to eliminate background noise. Mean computation time on a 256×256 image is around 4.5 seconds using either the automatic or the semi-automatic approach with non-optimized Matlab code running on an Intel Core 2 Duo 2.53 GHz.

We evaluated the accuracy of our Vessel Walker (VW) method (using VW-A and VW-SA formulations) and compared it to Frangi's vesselness filter (VF) [3], the Random Walker (RW) algorithm [8] and an active contour-based (AC) method [6]. Table 3 shows the average precision, recall, Dice coefficient and area under the ROC curve (AUC), obtained on the 9 angiograms. To measure the precision, recall and Dice coefficient, segmented vessels were obtained by thresholding the vesselness values (Frangi) or the $\boldsymbol{f}$ values (RW and VW), and by comparing these segmentations to the ground truth. For Frangi and our VW method, Otsu's thresholding technique was used [12], while the prescribed threshold of 0.5 was used for RW. The results of Table 3 show that our method (using VW-A and VW-SA) offers a good compromise between the precision and recall, as indicated by the best Dice of 0.71 obtained by our semi-automatic method. Moreover, to avoid the potential bias of threshold selection, we generated receiver operating characteristic (ROC) curves by varying the threshold from 0 to 1, and calculated the average area under the curve (AUC) obtained on the 9 tested angiograms. As reported in Table 3, our semi-automatic method achieved the best performance, with an average AUC of 97.2%.

Figure 1 shows three angiograms and their corresponding segmentation (overlaid in yellow), obtained with the Active Contour method, the Random Walker algorithm, and our Vessel Walker approach (using the automatic and semi-automatic

	VF [3]	AC [6]	RW [8]	VW-A	VW-SA
Precision	0.77	0.68	0.40	0.60	0.66
Recall	0.35	0.54	0.83	0.72	0.79
Dice	0.46	0.58	0.52	0.63	0.71
AUC	0.95	0.93	0.92	0.96	0.97

Table 1. Average performance on the 9 angiograms, obtained by Frangi's filter, the Active Contour method, the Random Walker algorithm and our proposed method (both in the automatic and semi-automatic formulations)

formulations).

Both formulations of the proposed method show good qualitative results in extracting not only large coronary vessels but also small vessels with low contrast. The automatic formulation of our method brings satisfactory results in comparison with the RW and AC results. However, these results show false negative and false positive regions. The limitations of the automatic formulation can be corrected through the insertion of seeds as shown in the right-most column of the figure. Using the same seed points, however, the Random Walker algorithm failed to correctly extract the coronary arteries, due to leakage. In our method, this problem is avoided thanks to the vesselness priors. Due to the combination of vesselness and intensity information, our method shows less false negatives than the Active Contour method which relies only on intensity homogeneity to segment a region.

An example of Frangi's vesselness values and the f values obtained by our VW-SA method is given in Figure 2. Values from 0 to 1 are color-coded such that the lowest possible foreground probability is dark blue and the highest one is red. We notice that the proposed method provides a better separation between the foreground and background values, and that the arteries' lumen and bifurcations are more easily distinguishable.

4. CONCLUSION

We proposed a new interactive vessel segmentation method that extends the Random Walker formulation by integrating vesselness information. This method was tested on 2D X-ray coronary arteries angiographies and obtained more accurate results than the active contour-based method. As future works, we will evaluate the effect of seed point selection on the segmentation performance, and investigate the usefulness of other types of vesselness priors.

5. REFERENCES

[1] WorldHealthOrganization, "Cardiovascular diseases (cvds), fact sheet n317," September 2012.

[2] D. Lesage, E.D. Angelini, I. Bloch, and G. Funka-Lea, "A review of 3D vessel lumen segmentation techniques: Models, features and extraction schemes," *Medical Image Analysis*, vol. 13, no. 6, pp. 819–845, 2009.

[3] A.F. Frangi, W.J. Niessen, K.L. Vincken, and M.A. Viergever, "Multiscale vessel enhancement filtering," *MICCAI*, vol. 1496, no. 3, pp. 130–137, 1998.

[4] Y. Sato, S. Nakajima, N. Shiraga, H. Atsumi, S. Yoshida, T. Koller, G. Gerig, and R. Kikinis, "Three-dimensional multi-scale line filter for segmentation and visualization of curvilinear structures in medical images," *Medical Image Analysis*, vol. 2, no. 2, pp. 143–168, 1998.

[5] A. Vasilevskiy and K. Siddiqi, "Flux maximizing geometric flows," *Pattern Analysis and Machine Intelligence*, vol. 24, no. 12, pp. 1565–1578, 2002.

[6] F. M'hiri, N.L.T. Hoang, L. Duong, and M. Cheriet, "A new adaptive framework for tubular structures segmentation in x-ray angiography," in *Information Science, Signal Processing and their Applications (ISSPA), 2012 11th International Conference on*. IEEE, 2012, pp. 496–500.

[7] F. Benmansour and L. D. Cohen, "Tubular structure segmentation based on minimal path method and anisotropic enhancement," *Int. J. Comput. Vision*, vol. 92, no. 2, pp. 192–210, Apr. 2011.

[8] L. Grady, Y. Sun, and J. Williams, "Interactive graph-based segmentation methods in cardiovascular imaging," in *Handbook of Mathematical Models in Computer Vision*, pp. 453–469. Springer, 2006.

[9] M. Schaap, L. Neefjes, C. Metz, A. van der Giessen, A. Weustink, N. Mollet, J. Wentzel, T. van Walsum, and W. Niessen, "Coronary lumen segmentation using graph cuts and robust kernel regression," in *Information Processing in Medical Imaging*, 2009, pp. 528–539.

[10] M. Freiman, N. Broide, M. Natanzon, E. Nammer, O. Shilon, L. Weizman, L. Joskowicz, and J. Sosna, "Vessels-cut: A graph based approach to patient-specific carotid arteriesmodeling," in *Modelling the Physiological Human*, vol. 5903 of *Lecture Notes in Computer Science*, pp. 1–12. Springer, 2009.

[11] A. Hernández-Vela, C. Gatta, S. Escalera, L. Igual, V. Martin-Yuste, and P. Radeva, "Accurate and robust fully-automatic qca: Method and numerical validation," in *MICCAI*, 2011, vol. 6893, pp. 496–503.

[12] N. Otsu, "A threshold selection method from gray-level histograms," *Automatica*, vol. 11, no. 285-296, pp. 23–27, 1975.